20

Brain Stimulation of Comatose Patients: A Chaos and Nonlinear Dynamics Approach

ROBERT W. THATCHER

20.1 Introduction

A recent and important contribution to the neurophysiological bases of human consciousness lies in the application of the mathematics of nonlinear dynamics or chaos theory to human electrophysiology. Recently, Freeman (1987a; 1987b) has used chaos theory to model state changes in the electroencephalogram (EEG), in which a relatively small number of parameters can determine brain state from seizure, deep anesthesia, sleep, awakeness, etc. One advantage of the nonlinear dynamic models of neural networks is simplification, whereby a small number of parameter changes can result in large-system state changes that may involve billions of individually interacting elements (Thompson and Stewart, 1986). Another advantage is the consistency of mathematics from the laws of physics to the laws of biology in which common, and often poorly understood, phenomena are explained by a single mathematical model (Peitgen and Richter, 1986; Swinney, 1983; Swinney and Gollub, 1981; Swinney and Roux, 1984; Thompson and Stewart, 1986).

In this context this chapter examines the application of nonlinear dynamics to the identification of EEG features that may predict changes in brain state following brain stimulation in comatose patients. This work arises from the early work of Hassler and colleagues (Hassler, 1979; Hassler et al., 1969) and more recent efforts by Francis Cohadon and colleagues in Lyons, France, and by Hosobuchi and Yingling at the University of California, San Francisco, to awaken patients who have been comatose for more than 2 years. Preliminary studies by Cohadon and colleagues have reported the successive awakening of eight of 13 patients stimulated with brainstem- and thalamic-implanted electrodes. Hosobuchi and Yingling (personal communication, 1988) are attempting to replicate and extend the Cohadon results while exploring different stimulus parameters and electrode locations. These clinical trials are not only of considerable clinical importance but they also represent a rare opportunity to investigate the genesis and maintenance of human consciousness. In recognition of work performed at the University of

Maryland and the presence of a large EEG database from noncomatose and comatose patients (Thatcher et al., 1983, 1987, 1989, 1990), Drs. Hosobuchi and Yingling are collaborating with Drs. Thatcher, Geisler, and Sestokas of the Applied Neuroscience Laboratory at Shock Trauma (University of Maryland Medical Systems) to evaluate features of the EEG that help identify levels of awareness and predict transitions from coma to awareness. Such information may be useful, especially when the patient is behaviorally comatose and unresponsive to conventional neurological examination. The study is limited to patients with minimal damage to cortical and supporting structures, such as the basal ganglia and thalamus, because such patients, after the risk and expense of surgical intervention, have a reasonable chance of leading normal and productive lives once they are awakened from their comatose states (Thatcher et al., 1990).

Three critical areas of experimental design were used in this collaboration: (1) the use of nonlinear dynamics to identify EEG state changes that may characterize the transition from coma to wakefulness, (2) the anatomical location of electrodes, and (3) parameters of electrical stimulation.

The clinical importance of the research into brain stimulation of comatose patients is illustrated by the fact that in 1975 the total number of individuals who suffered head injury in the United States, due to all causes, was estimated to be approximately 8 million (Wilder, 1976). Of these individuals approximately 70% suffered only mild head injury, defined by a Glasgow Coma Score (GCS) equal to or greater than 13 and either no loss of consciousness (e.g., mild concussion) or a loss of consciousness of no longer than 20 minutes (Langfitt and Gennarelli, 1982; Thatcher et al., 1989). The remainder, or approximately 2 million people, suffered moderate to severe brain damage defined by much longer periods of unconsciousness and greater depths of unconsciousness, e.g., GCS between 3 and 12 (Wilder, 1976). The state of being comatose is typically defined as a GCS less than 6 or a patient who does not respond to command and is not aware of his or her surroundings, e.g., GCS between 3 and 6. Although prolonged coma is all too common, the majority of the severely injured who survive the initial few weeks after admission to the hospital eventually recover consciousness to the extent that they are aware of their surroundings and gain willful control over themselves. However, the steps from deep coma to intermediate coma to the twilights of awareness require considerable time with very specific stages of improvement along the way. Figure 20.1 shows the various levels of the GCS from which comatose patients gradually climb, achieving more and more mental competencies.

20.2 Measuring EEG Transitions from Coma to Awakeness

Our initial design was to use scalp-recorded EEG from individual patients whose EEG had been repeatedly measured as they progressed from deep coma (GCS 3 to 6) to intermediate coma (GCS 7 to 12), to awakeness (GCS 13 to 15). In this way we could identify EEG features that characterize the transition from coma to

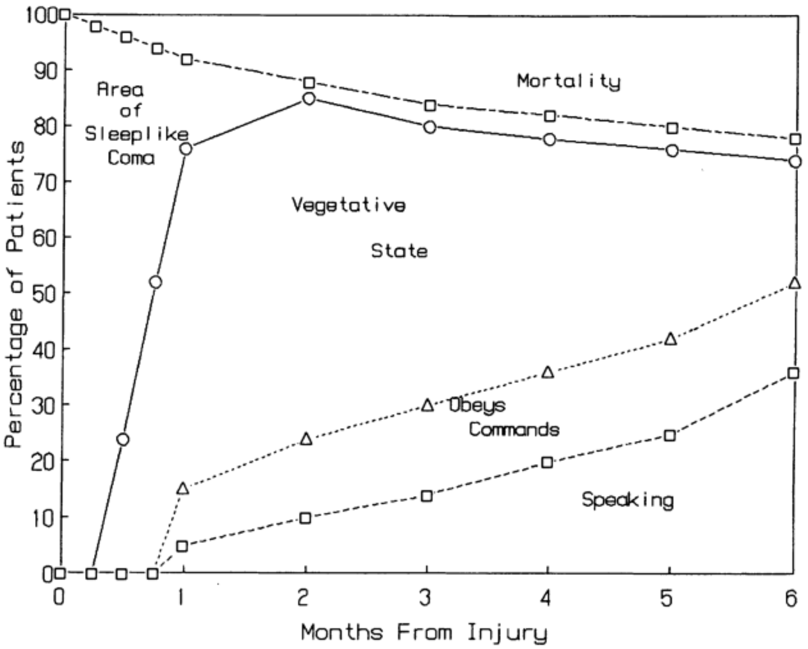

FIGURE 20.1. Time course of recovery of neurological functions in severely brain-injured patients. In general there is a shift from deep coma to a vegative state to a slow recovery of functions, such as obeying commands and speaking. The mortality rate tends to decrease as a function of time following injury.

awakeness and then empirically test nonlinear dynamical assumptions and models that may predict transitions of consciousness in comatose patients. We recognized that, even if a specific model were not derived, nonetheless, an empirical study of comatose patients' EEGs could help identify some of the practical steps necessary to eventually develop a nonlinear dynamical model. However, as of this date we have not completed the empirical aspect of this design. Therefore, this section only presents the general procedures and concepts that underlie nonlinear dynamical analyses of the human EEG. We consider these procedures as essential for the eventual empirical analyses.

20.2.1 EEG Synchrony versus Desynchrony

The human waking EEG is characterized by a narrow band spectrum with over 95% of the energy at frequencies ranging from near zero to approximately 30 Hz. For instance, in normal adult posterior cortex over 70% of the energy of the EEG is in the alpha band (e.g., 7 to 13 Hz), with a decreasing gradient extending anterior to about 45% at the frontal poles (John et al., 1980; Matousek and Petersen, 1973). The frequency spectrum of a normal adult typically exhibits a strong alpha peak (e.g., 10 Hz) with secondary peaks near the subharmonic and harmonic of the alpha frequency, e.g., near 5 Hz (theta band) and 20 Hz (beta band). The waking EEG is also characterized by intermediate bursts of synchronized rhythms embedded in a sea of desynchronized electrical activity with the interburst intervals occurring on a quasi-random basis (Freeman, 1987b). The EEG recorded during active tasks, for example, is characterized by a diminution in the number and amplitude of synchronized bursts and a general increase in desynchrony (Morrell, 1962). The spatial extent of the desynchronized EEG can also expand and contract depending upon the demands of the environment, such as in classic conditioning experiments (John, 1967; Morrell, 1962). Several studies have shown that diffuse and widespread EEG desynchronization observed during the initial stages of classic conditioning diminishes and contracts during the intermediate stages of conditioning to eventually become concentrated, like islands of desynchrony, in the neighborhood of the sensory and motor cortex involved in the mediation of the task. For example, persistent EEG desynchrony was confined either to the visual or auditory or somatosensory cortex depending upon whether the conditioned stimulus was, respectively, a visual or auditory or somatosensory stimulus (Gasteau et al., 1957).

In human EEG studies the power spectral measure called coherence is frequently used to measure the degree of desynchrony within and between regions of the human scalp. Coherence is mathematically analogous to a cross-correlation coefficient in the frequency domain (Bendat and Piersol, 1980) and provides information about the degree of coupling or shared activity between two spatially separate regions. There are two advantages of EEG coherence measures over other EEG measures: (1) coherence reflects the operation of the white matter of the neocortex through which cortico-cortical associations are made (Thatcher et al., 1986; Thatcher, 1990) and (2) coherence can be used to estimate such network properties as conduction velocity, frequency dispersion, direction vectors, and the magnitude of coupling (Bendat and Piersol, 1980). Consistent with the classic conditioning animal experiments, coherence measures of EEG synchrony in normal people have also shown certain systematic relationships. Figure 20.2 shows an example of the relationship between the magnitude of coherence and IQ in 199 children ranging in age from 5 to 16 years. This negative relationship between the magnitude of synchrony and intelligence was consistently observed in nearly all of the electrode pairs that were examined (Thatcher et al., 1983). Recently Rene Hernandes (1988) replicated this phenomenon in central, parietal, temporal, and occipital regions in an independent group of children. These findings were interpreted (Hernandes, 1988; Thatcher et al., 1983) in terms of information theory in which a desynchronized system represents a state of maximal readiness and maximal information capacity in an information theoretical sense (Shannon and Weaver, 1949).

20.3 Nonlinear Neural Network Models

Although the application of nonlinear dynamics to formulate models of human EEG is in a primitive stage of development, it may be helpful to briefly review

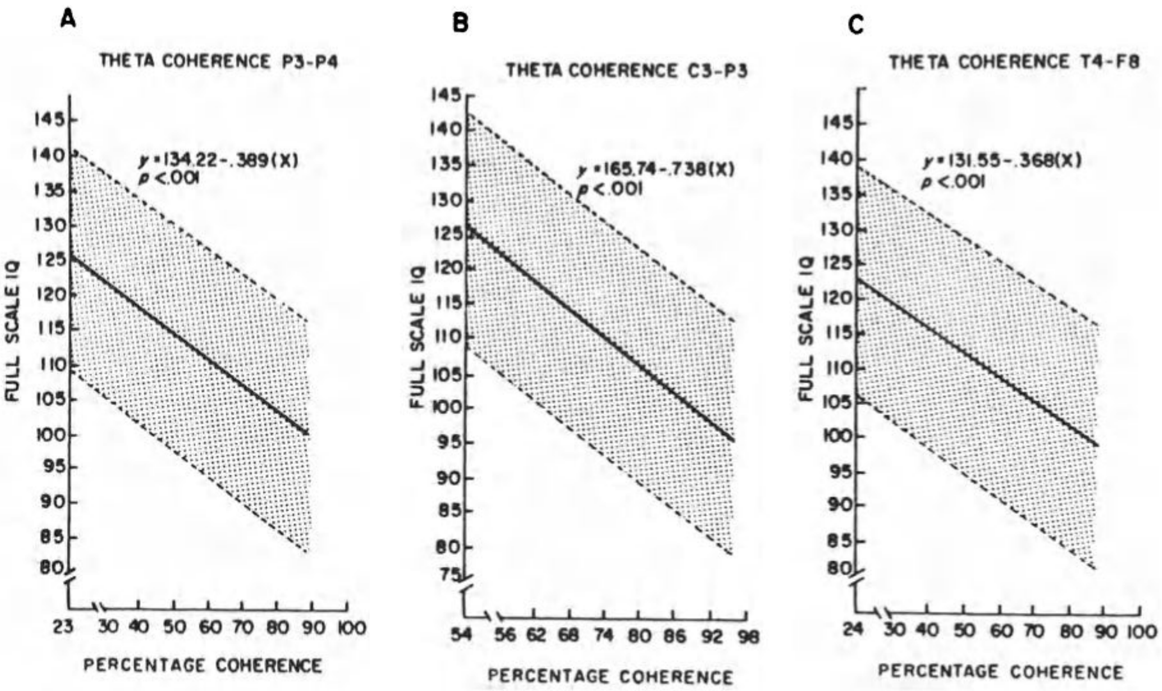

FIGURE 20.2. Polynomial regression analyses with full-scale IQ as the dependent variable and percentage coherence as the independent variable. A, Interhemispheric coherence between homologous parietal (P3 and P4) derivations. B, Left intrahemispheric coherence between left central (C3) and left parietal (P3) derivations. C, Right intrahemispheric coherence between the right anterior temporal (T4) and right frontal (F8) derivations. Dashed lines represent +– 1 S.E. Reprinted with permission from Thatcher et al. (1983): Hemispheric EEG asymmetries related to cognitive functioning in children. In: *Cognitive Processing in the Right Hemisphere,* A. Percuman, ed. New York: Academic Press.

some of the progress that has been made to date. The general feasibility of modeling EEG using ordinary differential equations (ODEs) was first demonstrated by Freeman (1975), who found that processes could be simulated that were statistically indistinguishable from real EEG. Nunez (1981) extended these efforts specifically to human EEG by taking into consideration variables such as skull volume, brain geometry, conduction velocities of cortical association fibers, and the distribution of short versus long distance cortico-cortical association fibers. Although both Freeman's and Nunez's models were nonlinear in nature, they were not specifically models of chaos.

The first neural network model of chaos was developed by Wilson and Cowen (1972, 1973). This is an important model because it is capable of exhibiting limit cycles that arise from a realistic neural network model. It has formed the foundation for a number of nonlinear dynamical neural models (see Kawahara, 1980; Skarda and Freeman, 1987) and is of considerable practical and historic relevance. The model contained two fundamental variables: the proportion of excitatory cells firing per unit time E(t) and the proportion of inhibitory cells firing per unit time T(t). We assume that E and I at time $(t+\tau)$ after a delay τ will be equal to the proportion of cells that are sensitive and also receive at least threshold excitation. Nonsensitive cells are those that, having recently fired, cannot fire again for their refractory period. Thus, if the absolute refractory period is r, the proportion of sensitive excitatory cells can be approximated:

$$E_s = 1 - r_e E$$

with a similar expression for I_s. The expected proportions of the subpopulations receiving at least threshold excitation per unit time will be a mathematical function of E and I, for which the proportion of excitatory cells is

$$\mathcal{L}(x) = \mathcal{L}[c_e E - g_e I + P(t)]$$

and for inhibitory cells is

$$\mathcal{L}(x) = \mathcal{L}[c_i E - g_i I + Q(t)]$$

Here, the coefficients are constants representing the average number of synapses per cell, and P(t) and Q(t) are external excitatory inputs.

After defining response functions (x), which depend on the probability distribution of neural thresholds (these are sigmoidal in shape), adjusting for coarse-graining assumptions and for a stable resting state condition, the following final differential equations were developed:

$$\tau_e \frac{dE}{dt} = -E + (k_e - r_e E)\mathcal{L}_e[c_e E - g_e I + P_{(t)}]$$

$$\tau_i \frac{dI}{dt} = -I + (k_i - r_i I)\mathcal{L}_i[c_i E - g_i I + Q_{(t)}]$$

With Q equal to zero and P equal to a certain constant value, the model can, with an appropriately chosen set of coefficients, exhibit a stable limit cycle as shown in Figure 20.3 (see Thompson and Stewart, 1986).

Recently, Kawahara (1980) extended this model to represent a system of mutually coupled Van der Pol equations. The issues of coupling coefficients and interconnectiveness within and between neural populations were addressed in this model. Thus, although a mature mathematic model has not yet been devised to describe the neurophysiological bases for the behavior of the EEG, considerable progress has nonetheless occurred (see also, Lopes de Silva et al., 1973).

Common features of all of these models are constants and coefficients that express the value of neural thresholds. Generally the thresholds depend on a probability distribution that has a sigmoidal shape, rising monotonically from zero and becoming asymptotic to a value equal to or near to unity. This aspect of the nonlinear modeling is relevant to the present discussion since it is known that the reticular activating system through its diffuse projection to the cortex and forebrain, can affect the neural thresholds in large populations of cells. Thus, electrical stimulation of the brainstem of comatose patients should have a profound effect on this important control parameter.

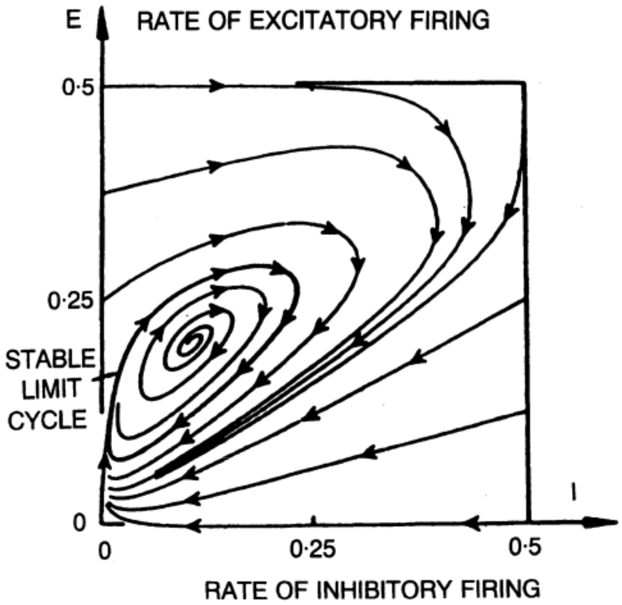

FIGURE 20.3. A stable limit cycle in the (E, I) phase space of a neural system. The limit cycle represents a steady oscillation in the two firing rates. Reprinted with permission from Thompson and Stewart (1986): *Nonlinear Dynamics and Chaos.* New York: John Wiley & Sons.

20.4 Nonlinear Dynamic Modeling of EEG

The role of EEG desynchrony in information processing has recently been mathematically modeled using nonlinear dynamics (Freeman, 1987a; Skarda and Freeman, 1987). Freeman and colleagues have shown that a bifurcation takes place when a neural system undergoes a major transition in its dynamics; for example, the transition from sleep to waking or from a normal waking state to seizure activity. These transitions are described by the language of nonlinear dynamics as a shift between two classes of attractors, e.g., from a limit cycle attractor to a chaotic attractor. The transition from a stable attractor to a chaotic attractor commonly involves a sequence of change from periodic motion to quasi-periodic motion to chaotic or nonperiodic motion, i.e., to a desynchronized state. According to this model, the state of chaotic EEG or desynchronized EEG is one of maximal information content, such as described in information theory (Shannon and Weaver, 1949). Skarda and Freeman (1987) argued that the state of chaos in neural networks constitutes a "ground state" or a condition of restless but bounded activity. This state resembles band-limited white noise; however, it is mathematically deterministic in the sense that it can be very simply and immediately turned on or off (Stewart and Thompson, 1986). In contrast to statistical randomness, which is determined by the central limit theorem, chaos is of a "low dimension" such that a small number of control parameters can significantly influence its presence or absence. For instance, Freeman (1987a) has estimated that the dimensionality of desynchronized EEG ranges from approximately 4 to 7. This low dimensional-control capability is ideal for any system that uses chaos in a functional sense frequently and with least effort. Changes in brain state from synchrony to desynchrony, for instance, are an example of where parametric control over chaos would be of biological importance.

Nonlinear dynamics can also be used to characterize EEG and single neuron behavior during the state transitions from sleep to dreaming to wakefulness, as well as during a pathological state, such as seizure or epilepsy. Figure 20.4 shows the behavior of pairs of individual neurons and the EEG during different stages of arousal in a rhesus monkey (Evarts, 1964), and Table 20.1 provides the nonlinear dynamical classifications. During waking a typically desynchronized EEG is present in Figure 20.4A with a seemingly random or unrelated time relationship between the spike discharges that emanated from the two neurons. Figure 20.4A shows that during waking the EEG is desynchronized, the interspike intervals for the two neurons are nonperiodic, and the cross-correlation between the two spike discharge time series is low. In terms of nonlinear dynamics the waking state is characterized by Chaotic-type behavior in all three times series measures. During slow wave sleep, in Figure 20.4B, the EEG exhibits increased synchrony, the interspike intervals show periodic burst patterns, and the cross-correlation between the two spike discharges is increased. In nonlinear dynamics terms the system is moving toward a limit cycle type of behavior in all three time series measures. The dreaming state is often referred to as the paradoxical sleep state since the EEG is desynchronized, the individual's eyes become extremely active, yet the threshold

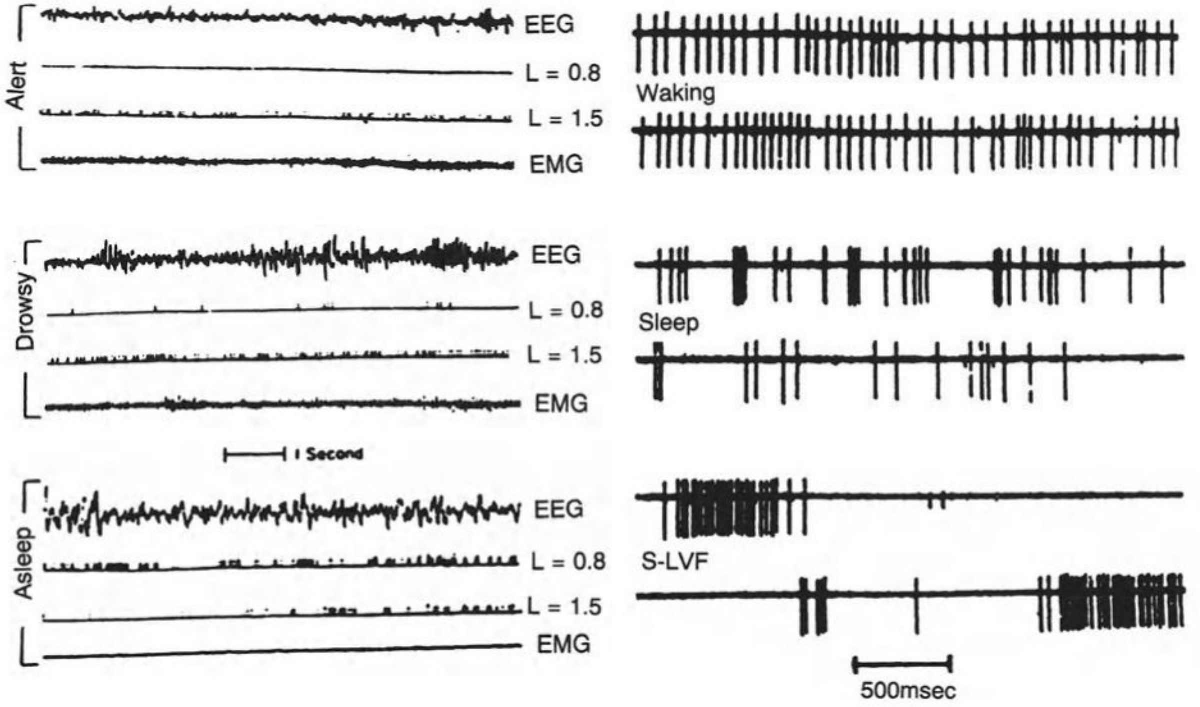

FIGURE 20.4. Patterns of unit discharge during waking, sleep (with EEG slow waves), and during paradoxical sleep (S-LVF). During waking, discharge tends to be regular with an absence of both short and long interspike intervals. During slow-wave sleep (*middle pair of traces*), there are bursts interspersed with periods of relative inactivity. With S-LVF, burst duration increases, intervening periods of inactivity become longer, and discharge frequency rises. The EEG is similar (low-voltage high-frequency activity) during waking and S-LVF. Note, however, that the pattern of discharge is markedly different during these two states. Reprinted with permission of the American Physiological Society from Evarts (1964): Temporal patterns of discharge of pyramidal tract neurons during sleep and waking in the monkey. *J. Neurophysiol.* 27: 152–171.

to awaken the individual is at its lowest. In Figure 20.4C, during dreaming or REM sleep the EEG is highly desynchronized; similar to the waking state, the interspike intervals are highly synchronized, even more than in the slow-wave sleep state, and the cross-correlation between the spike discharges is decreased. In nonlinear dynamics terms, during dreaming the EEG and the cross-correlation between spike trains are moving toward a Chaotic type of behavior while the interburst intervals move further toward the limit cycle type of behavior.

There are several generalizations that one may draw from these data. The first is that, because the cross-correlation between neurons (or the coherence) is the same in waking as it is in dreaming, one may conclude that critical parameters determining the transition from periodic-to-quasi-periodic-to-chaotic dynamics is the magnitude of coupling or forcing between neurons and the magnitude of coupling or forcing between neural networks. Therefore, such a coupling or forcing variable must be incorporated into any nonlinear dynamical model that purports to describe changes in brain state and in consciousness. The second is that the presence of the nonlinear transition sequences in brain state in Figure 20.4 and Table 20.1 helps narrow the search to identify the types of system behavior expected near the point of transition from periodic to chaotic. As Thompson and Stewart (1986) demonstrate mathematically, these behaviors can include intermittency, frequency locking, and period doubling. This indicates that one of the constraints on the development of a nonlinear model of consciousness would be that the model must account for the transition sequences actually observed in the human EEG as an individual changes brain state.

Table 20.1 Nonlinear Dynamical Associations During State Transitions*

Brain state	Nonlinear dynamic attractor type
Waking	EEG=quasi-periodic to chaotic
Waking	ISI=quasi-periodic to chaotic
Waking	Cross-correlation=low coupling
Slow-wave sleep	EEG=periodic (limit cycle)
Slow-wave sleep	ISI=periodic (limit cycle)
Slow-wave sleep	Cross-correlation=high coupling
Dreaming	EEG=quasi-periodic to chaotic
Dreaming	ISI=highly periodic (limit cycle)
Dreaming	Cross-correlation=low coupling
Seizure	EEG=highly periodic (limit cycle)
Seizure	ISI=highly periodic (limit cycle)
Seizure	Cross-correlation=high coupling

*Based on Freeman (1987a)
ISI=interspike interval.

20.5 How to Detect Chaos in the Human EEG

This section presents practical issues in the detection and analysis of nonlinear dynamical systems. Fortunately, high-speed computers and adaptable software have been developed to allow one to measure "chaos" in experimental data. An excellent software package for this purpose, which runs on an IBM-AT or compatible computer, was developed by Schaeffer et al. (1988). In order to facilitate the experimental application of the notions of nonlinear dynamics we draw explicitly on some of the features that have been made available by Schaeffer et al. (1988).

20.5.1 Power Spectral Analyses

An important practical question is how one goes about detecting chaos in the EEG and quantifying its transition states. The usual way of looking for order in a time series is to perform spectral analyses. Unfortunately, spectral analyses are not always a useful diagnostic tool for the detection of chaos. For example, Figure 20.5 shows power spectra for the Rossler attractor and the funnel (Schaeffer et al., 1988). Both of these attractors are chaotic and differ only in their parameter values, i.e., each has the same differential equations. However, in Figure 20.5A, we see very sharp spectral peaks, whereas in Figure 20.5B, there is a broad band and "featureless" spectrum. Farmer et al. (1983) have shown that the difference between these spectra is in the magnitude of "phase coherence." In Figure 20.5A, the cloud of initial points remains in phase with each other, even after many transits about the attractor. In contrast, in Figure 20.5B, the phase relationships of a set of initial points are rapidly destroyed, and the spectrum lacks prominent peaks. Thus, as Schaeffer et al. (1988) state, "The presence of sharp spectral peaks in a time series does not necessarily indicate a periodic attractor, nor does the absence of such peaks exclude the possibility of deterministic dynamics." In summary, caution must be exercised in relying solely upon power spectral analyses to analyze the nonlinear dynamics of the EEG.

20.5.2 The Phase Portrait

An especially useful diagnostic tool for analyzing nonlinear dynamical properties of a time series, such as an EEG, involves viewing the phase portrait. An important technical question is how one constructs phase portraits in cases where it is impossible to measure or know all of the state variables. As Schaeffer et al. (1988) point out, one can use Taken's method (Takens, 1980) of extracting the necessary information from a univariate time series. Takens (1980) showed that for any n-dimensional dynamical system for which measurements were made at t, t+T, t+2T, . . . for an observable y, then for almost any choice of y and time lag T, the phase portrait can be obtained by plotting:

$$y(t) \textit{ vs. } y(t+T) \textit{ vs } y(t+2T) \textit{ vs } \ldots . \; y[t+(m-1)T]$$

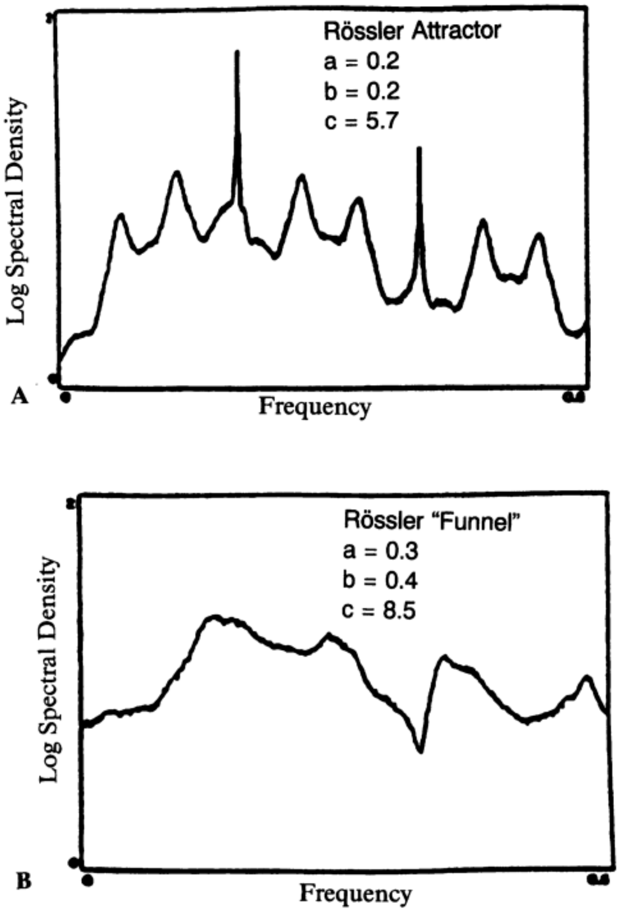

FIGURE 20.5. Phase-coherent (i.e., sharp spectral peaks) and phase-incoherent (i.e., weak or absent peaks) dynamics in Rossler's equations. A, The simple Rossler attractor. B, A variant on the funnel. Note the use of the log scale on the Y-axis. Reprinted with permission from Schaeffer et al., (1988): *Dynamical Software:* Vols I and II. Tucson: Dynamical Systems, Inc.

This is called "embedding" of the full *n*-dimensional system into a lower dimensional space. For practical purposes it is best to choose a time lag on the order of 10–30% of the period of an average orbital excursion. For spiky EEG data, a smaller lag may be necessary. It is important to emphasize, however, that the Takens method only provides a faithful reconstruction of the dynamical properties of the original time series. Thus, it is the dynamical properties, such as the fractal dimension, the Lyapunov exponents, etc., that must be emphasized. To be certain that the embedding process was conducted successfully, one should establish that the dynamical properties are indeed invariant with respect to the particular space in which the dynamics are represented or embedded.

20.5.3 Lyapunov Characteristic Exponents

The Lyapunov exponents measure the average rates at which nearby trajectories diverge or converge. This is an excellent method by which one examines the properties of an attractor. For example, for an attractor to be chaotic it must have at least one positive Lyapunov exponent. Mathematically, the Lyapunov exponents represent the rate and magnitude of deformation of a circle into an ellipsoid. For Lyapunov numbers greater than 1, the ellipsoid is expanding; numbers less than 1 imply contraction. For complete stability—the watershed between expansion and contraction—the number equals 0. Algorithms for computing Lyapunov exponents from experimental times series are given by Wolf et al. (1985) and Schaeffer et al. (1988). Figure 20.6 schematically shows the Wolf et al. (1985) method of computing the Lyapunov exponent.

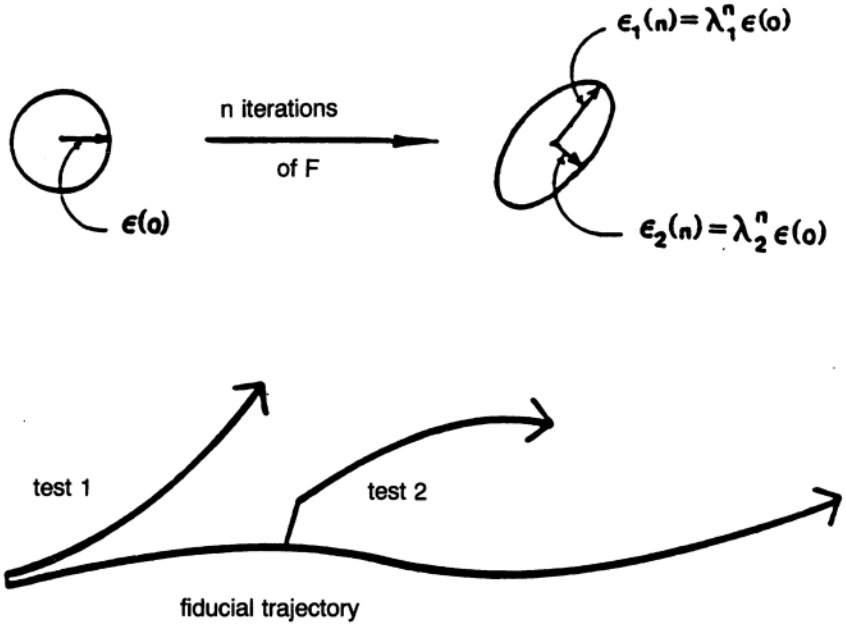

FIGURE 20.6. *Top,* Deformations of a circle of initial points into an ellipsoid. The Lyapunov numbers measure rates of expansion and contraction of the principal axes. For maps, Lyapunov numbers greater than 1 indicate expansion; numbers less than 1 imply contraction. For flows, the watershed between expansion and contraction is 0. In this case, one speaks of Lyapunov exponents. *Bottom,* Method used to estimate Lyapunov exponents. One begins by choosing a fiducial trajectory and a second nearby trajectory called the test trajectory. When the separation between the two trajectories becomes large, a new test trajectory is chosen at approximately the same distance and orientation as the first. When the equations of motion are known, this is accomplished by using (periodically renormalized) eigenvectors as test trajectories. For experimental data, one searches the data set for a suitable replacement. Reprinted with permission from Schaeffer et al. (1988): *Dynamical Software:* Vols I and II. Tucson: Dynamical Systems, Inc.

20.5.4 Kolmogorov-Sinai Metric Entropy

The metric entropy measures the average rate of information gained by measuring the neighborhood of a trajectory. The Kolmogorov-Sinai (K-S) metric is related to the Lyapunov exponent by equaling the sum of the positive Lyapunov exponents (Ruelle, 1983). In general, a positive K-S implies chaos. This follows from the fact that chaotic systems are sensitive to initial conditions, in which minute differences are eventually amplified to large-scale fluctuations. As a consequence, one can never predict the system's behavior into the indefinite future because one's predictions are degraded as one moves further into the future. The K-S metric measures the rate of information generation as the short-term predictability is transformed into long-term uncertainty. Based upon the methods of Schaeffer et al. (1988), the K-S entropy is computed by dividing the phase space into a minimal set of hypercubes sufficient to cover the attractor. Let p_i be the fraction of points that fall in the ith cube. Consider the quantity

$$I_{(e)} = -\sum_{i} P_i \log p_i$$

where e is the length of a side of the cube and $I(e)$ is information as defined by Shannon and Weaver (1949). From this one can define the information dimension as

$$d_i = \lim_{e \to 0} \; [I(e)/ln\,(1/e)]$$

To define the K-S entropy, space-time is divided into n bins of length e. Let p (i1, . . . in) be the joint probability that x(t+dt) falls in cube i1, x(t+2dt) in cube i2, . . . , x(t+n dt) in cube n. Then we can define

$$\tilde{I}(e) = -\sum_{i} p(il, \ldots, in)\; ln\; p(il, \ldots, in)$$

and the metric entropy as

$$\text{K-S} = \lim_{e \to 0} \; \lim_{n \to \infty} \; (1/n)\, \tilde{I}(e)$$

20.5.5 Fractal Dimension

A fractal dimension is where successive magnifications of a system reveal structure within structure, within structure . . . ad infinitum. Whereas the Lyapunov exponents measure the separation of neighboring trajectories, the fractal dimension is defined with respect to particular portions of phase space. Similar to the K-S entropy, one computes the fractal dimension by dividing the phase space into hypercubes and retaining a minimal set that covers the attractor. However, caution should be exercised because chaotic systems do not always have a noninteger or fractal dimension (Grebogi et al., 1984).

There are a great many different dimension-like quantities published in the fractal literature (Farmer et al., 1983; Grassberger and Procaccia, 1983a and b; Mandelbrot, 1977; Schaeffer et al., 1988). In general, these dimensions fall into two classes: metric dimensions and probabilistic dimensions. Metric dimensions are independent of the frequency with which various regions of the attractor are visited, whereas probabilistic dimensions explicitly utilize the frequency distribution, sometimes called the natural measure of the attractor. If the data under study constitute a known set, such as the long-term dynamics of a system of equations, then the metric and probabilistic dimensions are comparable (Farmer et al., 1983; Schaeffer et al., 1988). However, for experimental data, such as the EEG, the probabilistic dimension is easier and more accurate to estimate (Schaeffer et al., 1988). An example of a probabilistic fractal dimension that is related to the Lyapunov exponent is the dimension-like quantity called the Lyapunov dimension, *d*, as defined by the equation:

$$d_L = j + \Sigma\, i/ \quad | \quad j + i \;|$$

where the λ's are the Lyapunov exponents arranged in order of decreasing magnitude and *j* is chosen so that

$$\sum^{j-} \lambda_i > 0$$

$$\sum^{j+1} \lambda_i < 0$$

If *D* is a intermediate value between integers (e.g., 2.47), then we can expect to observe fractal structure in lower-dimensional maps (Schaeffer et al., 1988).

Another and more computationally efficient method of estimating the fractal dimension of a time series is that proposed by Grassberger and Procaccia (1983a and b). In their algorithm one replaces cube counting with the measurement of distances by computing the distance between all points of a time series and then asking what fraction is less than a series of predetermined length scales. The average of these lengths is defined as the correlation integral for different length scales, g. For example

$$C(g) = \lim_{N \to \infty} \quad \{1/[N\,(N\text{-}1)]\,\} \;\sum_{i,j} H\,(g,\, D_{ij})$$

where D_{ij} is the distance between points X and X , and *H (g, D)* is the Heaviside function

$$H\,(g,D) = \begin{cases} 0, & g < D \\ 1, & g > D \end{cases}$$

$C(g)$ increases from zero for g very small to 1 for g very large. Grassberger and Procaccia (1983a and b) show that for small g

$$C(g) \sim g^{h}$$

and the exponent, n, is a lower bound on the information dimension. In more detail, they propose that

$$n < d_I < d_H$$

where d_H is the Hausdorf dimension and the exponent, n, is referred to as the correlation dimension. Freeman (1987a) successfully used the Grassberger and Procaccia (1983a and b) method to measure the fractal or chaotic dimension of olfactory EEG yielding values between 4 and 7.

20.6 The Torus Route to Chaos in Periodically Forced Systems

As stated previously, it is presumptuous to assume that a mature nonlinear model of brain state control can be developed today. However, of the various nonlinear dynamical models available, the toroidal flow model represents a class of models that seem most appropriate for the brain stimulation experiments that are to be conducted on comatose patients. The torus is a reasonable model to start with because toroidal flow is produced when a system that oscillates on its own is subjected to periodic forcing at a different frequency. If we assume that comatose patients exhibit naturally oscillating neural systems (e.g., EEG), then brain stimulation at periodic intervals and/or periodic frequencies and/or at periodic intensities may produce dynamic toroidal behavior.

By toroidal behavior we mean the motion of trajectories on the surface of a torus, i.e., a doughnut. Toroidal motion contains two classes of dynamics: (1) the motion is periodic in which the orbit winds around the torus an integer number of times before repeating itself, and (2) the motion never repeats itself and in fact covers the entire surface of the torus. In the first case the motion is said to be phase-locked, and in the second it is said to be quasi-periodic. As shown by Thompson and Stewart (1986), a change in parameter value of a dynamical system often results in the following sequence:

Limit Cycle → Quasi-periodicity
Limit Cycle → Phase Locking
Limit Cycle → Chaos

A frequently used mathematical model of toroidal flow is the following system of equations:

$$dx/dt = f(x, y, u)$$

$$dy/dt = g(x, y)$$

where $f(x,y,u)$ and $g(x,y)$ are nonlinear functions and $u=u(t)$ is a periodic function of time with period T. In this model there are two frequencies of interest: the inherent frequency of the nonlinear oscillator and the forcing frequency. As mentioned above, the inherent frequency of the system can represent the background EEG and/or sleep-wakefulness cycle of the comatose patient, and the second forcing frequency can represent various stimulus parameters used to awake the patient.

Although there are many ways to analyze this system of equations, one of the more interesting is to plot x and y at intervals equal to the period, T, of forcing. The resulting construction is called a time-one map or a Poincare map. The time-one map will be a closed curve topologically equivalent to a circle. In order to represent the positions of successive points, Schaeffer et al. (1988) introduced a construction called a circle map, which gives the sequence of rotations on the torus. This map, which is shown in Figure 20.7, is produced as follows:

Impose coordinate axes at the "center of mass."
To each point, *i*, assign an angle, $y(i)$.
Plot the y's in temporal sequence, i.e., for all pairs of points, *i* and *i*+1, plot $y(i+1)$ vs. $y(i)$.

The rotations on the torus are defined for the ith rotation as

$$r(\mathrm{i}) = y(i + 1) - y(i)$$

This allows us to compute the so-called rotation number r, which is simply the long-term average of the individual rotations:

$$r = \lim_{n\to\infty} \frac{1}{n} \sum_{i} \frac{r(i)}{2\pi}$$

Thus, if the average number of rotations is 360° then $r=1$.

20.7 Where Should the Electrodes Be Placed?

It is obvious that there is a limit to the number of brain-stimulating electrodes that can be placed in a comatose patient. A subset of candidate brain regions that are likely to have a low threshold for activation must be selected. The following sections review some of the literature concerning possible neuroanatomical control networks responsible for the sleep-wakefulness cycle and the known inhibitory and facilitatory brainstem and forebrain regions.

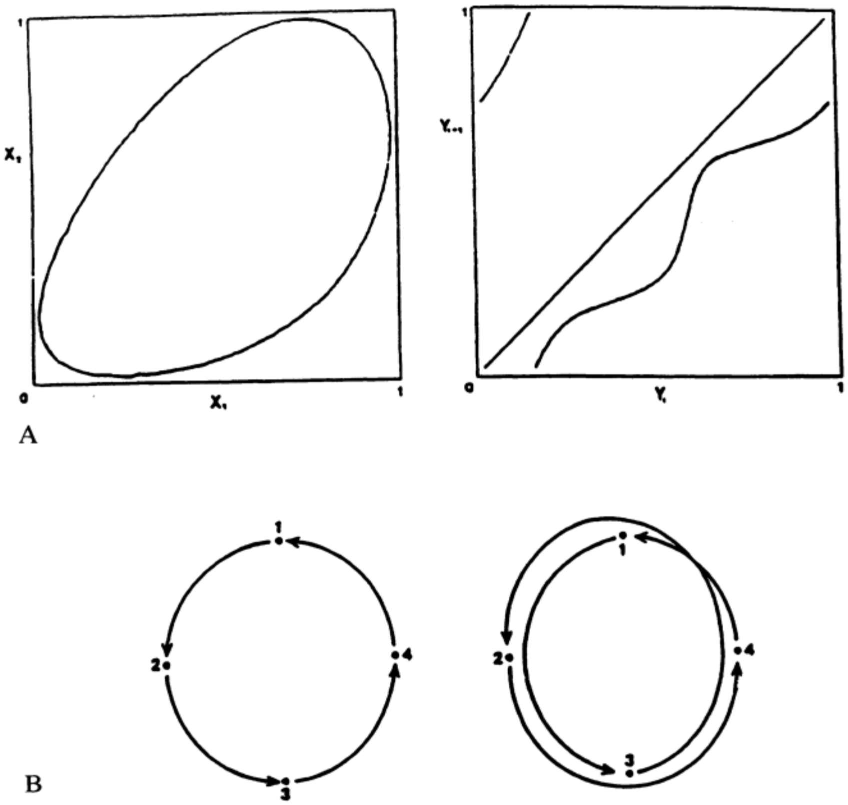

FIGURE 20.7. A, Invariant circles and circle maps. *Left,* For quasi-periodic motion, the time-one map is a closed curve topologically equivalent to a circle. The lines indicate the sequence of points. *Right,* A circle map is constructed by imposing coordinate axes at the center of mass (marked with a cross) of the invariant circle and assigning an angle, y(i), to each point. One then plots y(i+1) versus y(i) for all pairs, i and (i+1). B, For periodic orbits, the rotation number, r, is simply the number of rotations required to visit all points on the time-one map divided by the number of points. *Left,* r=1/4=0.25. *Right,* r=2/4=0.5. Reprinted with permission from Schaeffer et al. (1988): *Dynamical Software:* Vols I and II. Tucson: Dynamical Systems, Inc.

20.7.1 Sleep-Wakefulness Control Systems

An understanding of some of the anatomical systems involved in the regulation of sleep, wakefulness, and arousal states has come about through the use of three techniques: electrical brain stimulation, brain lesions, and neurochemical manipulations. For example, relatively low levels of high-frequency stimulation in the midline thalamus and reticular formation can transform a sleeping animal whose EEG is dominated by slow waves to one displaying an activated EEG and behavioral arousal. This effect is mediated largely by excitatory drives exerted on cortical, limbic, and basal ganglia structures (Thatcher and John, 1977). Lesions of the mesencephalic and pontine reticular formation result in a comatose state, characterized by a slow-wave EEG at intermediate levels of coma to a disorganized and low-amplitude EEG at deep coma (Bricolo et al., 1978). The symptoms of the sleeping disease—encephalitis lethargical (Economo, 1918)—are largely the result of lesions in the central gray of the brainstem. Similarly, tumors in this region produce prolonged states of somnolence (Fulton and Bailey, 1929).

These classic findings, which constituted an important contribution to the development of contemporary neuroscience, led to the formulation of the concept of an ascending reticular activating system involved in the control of sleep-wakefulness (Lindsley et al, 1949; Moruzzi and Magoun, 1949). Damage to the sensory-specific systems had little effect on sleep-wakefulness, whereas lesions located a few centimeters more medially would produce a depressed, somnolent state.

The possibility of reciprocal corticoreticular influences on the control of arousal was demonstrated through electrical stimulation studies by French, Hernandez-Peon, and Livingston in 1955. Lindsley (1950) was one of the first to emphasize the role of descending cortical influences in the control of arousal and attention, as well as in emotion and motivation. The recognition that the limbic system and cortex-made contributions to the reticular formation made it possible to conceive of how internal states, such as thoughts, worries, and apprehensions, might generate arousal activity in the reticular formation.

Further emphasis on reciprocal and dynamic control mechanisms in the regulation of sleep-wakefulness was provided by the finding that sleep can be produced not only by the reduction of activity in a tonic activating system but also by the influence of an active sleep-producing system. Hess (1954) and others (Akimoto et al., 1956; Hess et al., 1953) demonstrated that low-frequency stimulation of diencephalic structures would cause otherwise alert cats to select a likely place, after which they would curl up and then proceed to go to sleep much as a normal animal. In a study of the hypothalamic region of rats, Nauta (1946) found that lesions of the posterior thalamus produced prolonged somnolence, whereas lesions of more anterior hypothalamic regions produced rats incapable of sleeping. These results fit in with the findings of Economo (1918) who found, in some encephalitic patients, prolonged sleeplessness associated with lesions in the anterior hypothalamus.

More recent studies have mapped out the areas within the hypothalamus, limbic system, and reticular formation involved in the control of sleep and wakefulness (Hernandez-Peon and Chavez-Ibarra, 1963; Hernandez-Peon et al., 1963; Jouvet, 1969). Hypnogenic regions have been found throughout the pons, upper mesencephalon, diencephalon, and limbic system, as well as the orbital frontal cortex (Akert et al., 1952; Hess, 1954). A reciprocal activation-suppression relationship exists within the pontine reticular formation. Batini et al. (1959) demonstrated that lesions of the rostral pons gave rise to an EEG picture of arousal, whereas lesions a few millimeters lower, at the midpontine level, resulted in an EEG pattern typical of sleep. The inference drawn from these studies was that a mechanism present in the lower part of the reticular formation brings about sleep by inhibiting the upper reticular formation (Moruzzi, 1960). This inference was supported by experiments that blocked the upper and lower brainstem structures separately through the perfusion of barbiturates in the carotid and vertebral arteries, respectively (Magni et al., 1959). Perfusion of the caudal half of the brainstem through the vertebral arteries resulted in activation of the EEG, whereas barbiturate perfusion of the upper portion via the carotids resulted in a sleep-like EEG.

These data support a oscillatory model of brain-state control and regulation in which at least two systems are involved and distributed within both diencephalic-limbic and reticular formation structures, one a sleep-producing or hypnotic system, and the other an awakening or arousal system. These systems appear to be reciprocally connected so that activity in one will suppress the other and vice versa, thus giving rise to the sleep-wakefulness cycle (Hernandez-Peon and Chavez-Ibarra, 1963). This substrate of a reciprocally connected control circuit is typical of many neurophysiological systems (Thatcher and John, 1977).

20.7.2 Reticular and Diencephalic Facilatory-Inhibition Centers

Some of the dynamic reciprocal control centers in the diencephalon and brainstem are shown diagrammatically in Figure 20.8. This set of relations (pluses representing facilatory outflows and minuses representing inhibitory influences) was discovered by Magoun and collaborators (Bach & Magoun, 1947; Lindsley et al., 1949; Magoun & Rhines, 1948). These workers demonstrated that, when stimulated, the rostral portion of the reticular formation (involving mesencephalon and pontine regions labeled as structure 5 caused facilitation or enhancement of spinal reflexes and cortically initiated movement. This was also the region of lowest threshold for arousal and therefore should be a major candidate for deep brain stimulation in comatose patients. A second, more dorsal facilitatory region (labeled 6) is related to the vestibulospinal system. Stimulation of this system affects tonic facilitatory mechanisms involved in the control of posture. In contrast, stimulation of area 4 (caudal reticular formation) results in an inhibitory effect on spinal motor outflow and has been shown to reduce spasticity and hyperreflexia. Stimulation of the other inhibitory regions (1, 2, or 3) reinforces the suppressor or inhibitory role of the caudal reticular formation. Lesions of the inhibitory regions result in increased spasticity or hyperreflexia due to the dominance of the facilitatory reticular formation system. Thus, it appears that an appropriate balance between inhibition and facilitation can be maintained by such a mechanism, with the normal state of a waking animal favoring facilitation of spinal reflexes and motor outflows. In relation to drowsiness or sleep, there is a progressive tendency for the inhibitory system to dominate, resulting in sluggish reflexes and loss of postural control.

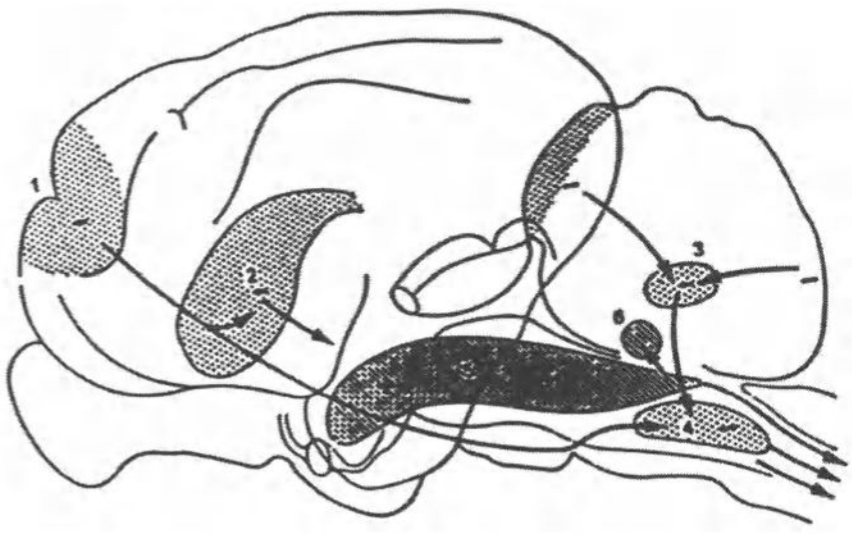

FIGURE 20.8. Excitatory and inhibitory influence of stimulation of the nuclei of the reticular formation: (5) and (6) facilatory, and (4) inhibitory zones of the brainstem reticular formation and connections running to it from the cortex (1), thalamus (2), and cerebellum (3). Reprinted with permission from Luria (1973): *The working brain.* Middlesex, England: Penguin Press.

This complex set of interrelationships reveals a system with enormous capabilities for the regulation of levels of arousal. First, the system possesses wide-ranging ascending influences so that its outflow can modulate the level of excitation of extensive regions of the cortex. In the case of absent or diminished outflow, the tonic level of cortical excitability will drop. Second, the inputs to this system from relay nuclei, limbic system, and cortex can act upon it so as to cause alterations in the level of arousal. Finally, outputs from this system to structures that are possible sources of such inputs provide the capability of fine adjustments, increasing the effectiveness of particular inputs so small changes in afferent intensity will cause major changes in arousal level, or decreasing the effectiveness of other inputs so they are temporarily excluded from acting upon the system.

20.8 The Parameters of Brain Electrical Stimulation

We come finally to the question of what are the best stimulus parameters, e.g., stimulus duration, stimulus intensity, on-off cycles, etc. It should now be clear that the critical observation concerns the neural dynamics during the transition from one brain state to another. Careful monitoring of the comatose patient's EEG is essential in order to describe the time series events preceding, during, and following changes in brain stimulation. If we follow a simple toroidal model of forced oscillations, then we should look for periodic, quasi-periodic, phase locking, and chaotic behaviors in the EEG, which are deterministically related to the stimulus parameters. Thus, it is desirable to record from as many electrodes as possible, including the stimulating electrodes (i.e., during the pre-and poststimulation periods to detect afterdischarges) with a high enough sampling rate (e.g., greater than 1000 Hz) to resolve spike discharges and rapid bifurcations.

Brain stimulation studies of comatose cats have shown that brief but daily stimulation of brainstem locations with low arousal thresholds was optimal in awakening the animal (see Chapter 3). Because these studies were conducted on surgically lesioned animals it was possible to determine the arousal thresholds before brain surgery. Obviously, this is not possible in brain-injured comatose patients. However, the power spectrum of the cortical EEG can reveal a circadian pattern or oscillatory pattern of changes in cortical excitability. The idea is to use these measure to deliver electrical stimulation when the patient is most aroused.

In the Cohadon preliminary studies, daily stimulation of the nucleus centrum median was used without systematic exploration of optimal stimulus parameters. However, Drs. Hosobuchi and Yingling used a 20-channel EEG and evoked potential system to record from scalp and deeply implanted electrodes. This system allows them to evaluate stimulus intensity thresholds for afterdischarge and maximum effect on the arousal pattern of the cortical EEG. That is, they can quantify the magnitude of change in EEG delta and alpha activity produced by different stimulus parameters, such as stimulus frequency, stimulus duration, and stimulus intensity, and then utilize the most effective stimulus settings.

20.9 Discussion

In theory it should be possible to obtain estimates of the dimensions of nonlinear dynamics of the cortical and subcortical EEG that are correlated with the recovery process in comatose patients and that characterize state changes that are parallel to or accompany changes in levels of awareness. Although this experimentation may not provide a mathematical model of consciousness, it nonetheless should add to our understanding of some of the dynamical neurophysiological processes that accompany the transition from coma to awakeness. An accurate nonlinear dynamical analysis may aid in the development of mathematical models of brain-state properties, such as stability and instability, expansion and contraction, excitation and inhibition, competition and cooperation, and the creation, transition, and destruction of brain states. It may provide clues to the critical dimensionalities that are relevant to the process of consciousness and point toward future experimentation to reveal more about the underlying neurophysiology. In a practical sense, a mature nonlinear dynamical model of brain-state changes may aid in the remediation of neurological disorders by providing reliable predictors in patients who are comatose and unable to respond to conventional neurological and neuropsychological evaluation. In the present context, such a model may guide experimental procedures to identify the optimal stimulus parameters and electrode locations used in the brain stimulation of comatose patients.

Acknowledgments. I would like to thank Dr. Anthony Sestokas for his interest and enthusiasm regarding collaboration in the study of brain stimulation of comatose patients and his approval and encouragement for the collaboration between the Shock Trauma Neurometrics Laboratory and Drs. Hosobuchi and Yingling at the University of California. The Shock Trauma patient EEG data that were used to begin the nonlinear dynamical analyses were collected while I was the Principal Investigator and/or the Scientific Director of the UMES-Shock Trauma Neurometric Clinical service. I also acknowledge Dr. Fred Geisler who gave permission for access to the neurotrauma EEG data as the physician of record of the neurotrauma patients.

References

Akert, K., Koella, W., Hess, R. (1952): Sleep produced by electrical stimulation of the thalamus. *Am. J. Physiol.* 168, 260–267

Akimoto, H., Yamaguchi, N., Okabe J., Nakagawa, T., Nakamura, I., Abe, K., Torri, H., Masahashi, K. (1956): On sleep induced through electrical stimulation of dog thalamus. *Folia. Psychiatry Neurol.* 10, 117–146

Bach, L., Magoun, H.W. (1947): The vestibular nuclei as an excitatory mechanism for the cord. *J. Neurophysiol.* 5, 331–337

Batini, C., Moruzzi, G., Palestini, M., Rossi, G., Zanchetti, A. (1959): Effects of complete pontine transections on the sleep-wakefulness rhythm: The midpontine pretrigeminal preparation. *Arch. Ital. Biol.* 97, 1–12

Bendat, J.S., Piersol, A.G. (1980): *Engineering applications of correlation and spectral analysis.* New York: John Wiley & Sons

Bricolo, A., Turazzi, S., Faccioli, F., Odorizzi, F., Sciarretta, G., Erculiani, P. (1978): Application of compressed spectral array in long-term EEG monitoring of comatose patients. *Electroenceph. Neurophysiol.* 45, 221–225

Economo, C. Von. (1918): *Die Encephalitis Lethargica.* Vienna: Deuticke. Cited in Ochs, S. (1965): *Elements of neurophysiology.* New York: John Wiley & Sons

Evarts, E.V. (1964): Temporal patterns of discharge of pyramidal tract neurons during sleep and waking in the monkey. *J. Neurophysiol.* 27, 152–171

Farmer, J.D., Ott, E., Yorke, J.E. (1983): The dimension of chaotic attractors. *Physica* 7D, 153–180

Freeman, W.J. (1975): *Mass action in the nervous system.* New York: Academic Press

Freeman, W.J. (1987a): Simulation of chaotic EEG patterns with a dynamic model of the olfactory system. *Biol. Cybern.* 56, 139–150

Freeman, W.J. (1987b): Analytic techniques used in the search for the physiological basis of the EEG. In: *Methods of analysis of brain electrical and magnetic signals. EEG handbook (revised series, vol. 1).* Gevins, A.S., Remond, A. (eds.). Amsterdam: Elsevier

Fulton, J.F., Bailey, P. (1929): Tumors in the region of the third ventricle: Their diagnosis and relation to pathological sleep. *J. Nerv. Ment. Dis.* 69, 1–25

Gasteau, H., Jus, A., Jus, C., Morrell, F., Storm Van Leewen, W., Dongier, S., Naquet, R., Regis, H., Roger, A., Bekkering, D., Kamp, A., Werre, J. (1957): Etude topographique des reactions electroencephalographiques conditioness chez l'homme. *Electroenceph. Clin. Neurophysiol.* 9, 1–14

Grassberger, P., Procaccia, I. (1983a): Characterization of strange attractors. *Phys. Rev. Lett.* 50, 346–249

Grassberger, P., Procaccia, I. (1983b): Measuring the strangeness of strange attractors. *Physica* 9D;, 189–208

Grebogi, C., Ott, E., Pelikan, S., Yorke, J.A. (1984): Strange attractors that are not chaotic. *Physica* 13D, 261–268

Hassler, R. (1979): Striatal regulation of adverting and attention directing induced by pallidal stimulation. *Appl. Neurophysiol.* 42, 98–102

Hassler, R., Dalle, G., Bricolo, A., Dieckmann, G., Dolce, G. (1969): Behavioral and EEG arousal induced by stimulation of unspecific projection systems in a patient with post-traumatic apallic syndrome. *Electroenceph. Clin. Neyurophysiol.* 27, 306–310

Hernandez, R.S. (1988): *The effects of task condition on the correlation of EEG coherence and full-scale IQ.* Doctoral dissertation, Maharishi International University, India

Hernandez-Peon, R., Chavez-Ibarra, G. (1963): Sleep induced by electrical or chemical stimulation of the forebrain. *Electroenceph. Clin. Neurophysiol.* 24 (Suppl.), 118–198

Hernandez-Peon, R., Chavez-Ibarra, G., Morgane, P.J., Timo-Iaria, C. (1963): Limbic cholinergic pathways involved in sleep and emotional behavior. *Exp. Neurol.* 8, 93–111

Hess, R., Koella, W.P., Akert, K. (1953): Cortical and subcortical recordings in natural and artificially induced sleep in cats. *Electroenceph. Clin. Neurophysiol.* 5, 75–90

Hess, W.R. (1954): *Diencephalon-autonomic and extra-pyramidal functions.* New York: Grune & Stratton

John, E.R. (1967): *Mechamisms of memory.* New York: Academic Press

John, E.R., Ahn, H., Prichep, L., Trepetin, M., Brown, D., Kaye, H. (1980): Developmental equations for the EEG. *Science* 210, 1255–1258

Jouvet, M. (1969): Biogenic amines and the states of sleep. *Science* 163, 32–41

Kawahara, T. (1980): Coupled Van der Pol oscillators: A model of excitatory and inhibitory neural interactions. *Biol. Cybernet.* 39, 37–43

Langfitt, T.W., Gennarelli, T.A. (1982): Can the outcome from head injury be improved? *J. Neurosurg.* 56, 19–25

Lindsley, D.B. (1950): Emotions and the electroencephalogram. In: *Feelings and emotions: The Mooseheart Symposium.* Reymert, M.L. (ed.). New York: McGraw-Hill

Lindsley, D.B., Schreiner, L., Magoun, H.W. (1949): An electromyographic study of spasticity. *J. Neurophysiol.* 12, 197–205

Lopes da Silva, F.H., Van Lierop, T.H., Schrijer, C.F., Storm van Leeuwen, W. (1974): Organization of thalamic and cortical alpha rhythms: Spectra and coherences. *Electroenceph. Clin. Neurophysiol.* 35, 627–639

Luria, A.R. (1973): *The working brain.* Middlesex, England: Penguin Press

Magni, F., Moruzzi, G., Rossi, G.F., Zanchetti, A. (1959): EEG arousal following inactivation of the lower brain stem by selective injection of barbiturate into lower brain stem circulation. *Arch. Ital. Biol.* 97, 33–46

Magoun, H.W., Rhines, R. (1948): *Spasticity: The stretch reflex and extrapyramidal systems.* Springfield, IL: Charles C. Thomas

Mandelbrot, B. (1977): *Fractals: Form, chance and dimension.* San Francisco: Freeman Publishing Co.

Matousek, M., Petersen, I. (1973): Frequency analysis of the EEG background activity by means of age dependent EEG quotients. In: *Automation of clinical electroencephalography.* Kellaway, P., Petersen, I. (eds.). New York: Raven Press

Morrell, F. (1962): Electrophysiological contributions to the neural basis of learning. *Physiol. Rev.* 41, 443–476

Moruzzi, G. (1960): Synchronizing influences of the brain stem and the inhibitory mechanisms underlying the production of sleep by sensory stimulation. *The Moscow Colloquim on Electroencephalography of Higher Nervous Activity, Electroencephalography and Clinical Neurophysiology* 13, 231–256

Moruzzi, G., Magoun, H.W. (1949): Brain stem reticular formation and activation of the EEG. *Electroenceph. Clin. Neurophysiol.* 1, 455–473

Nauta, W.J.H. (1946): Hypothalamic regulation of sleep in rats: An experimental study. *J. Neurophysiol.* 9, 285–316

Nunez, P. (1981): *Electric fields of the brain: The neurophysics of EEG.* New York: Oxford University Press

Peitgen, H.O., Richter, P.H. (1986): *The Beauty of fractals.* New York: Springer-Verlag

Ruelle, D. (1983): Five turbulent problems. *Physica* 7D, 40–44

Schaeffer, W.M. Truty, G.L., Fulmer, S. (1988): *Dynamical software: vols. I and II* Tucson: Dynamical Systems, Inc.

Shannon, C.E., Weaver, W. (1949): *The mathematical theory of communication.* Urbana, IL: University of Illinois Press

Skarda, C.A., Freeman, W.J. (1987): How brains make chaos in order to make sense of the world. *Behav. Brain Sci.* 10, 161–195

Swinney, H.L. (1983): Observations of order and chaos in nonlinear systems. *Physica* 7D, 3–15

Swinney, H.L., Gollub, J.P. (eds.). (1981): *Hydrodynamic instabilities and the transition to turbulence.* New York: Springer-Verlag

Swinney, H.L., Roux, J.C. (1984): Chemical chaos. In: *Nonequilibrium dynamics in chemical systems.* Vidal, C. (ed.). New York: Springer-Verlag

Takens, F. (1980): Detecting strange attractors in turbulence. In: *Dynamical systems and turbulence.* In: *Springer lecture notes in mathematics,* vol. 898. Rand, D.A., Young, L.S. (eds.). New York: Springer-Verlag, pp. 366–381

Thatcher, R.W., John, E.R. (1977): *Functional neuroscience: vol. I. Foundations of cognitive processes.* Hillsdale, NJ: Erlbaum Associates

Thatcher, R.W., McAlaster, R., Lester, M.L., Horst, R.L., Cantor, D.S. (1983): Hemispheric EEG asymmetries related to cognitive functioning in children. In: *Cognitive processing in the right hemisphere.* Perecuman, A. (ed.). New York: Academic Press

Thatcher, R.W., Krause, P., Hrybyk, M. (1986): Corticocortical association fibers and EEG coherence: A two compartmental model. *Electroenceph. Clin. Neurophysiol.* 64, 123–143

Thatcher, R.W., Walker, R.A., Giudice, S. (1987): Human cerebral hemispheres develop at different rates and ages. *Science* 236, 1110–1113

Thatcher, R.W., Walker, R.A., Gerson, I., Geisler, F.H. (1989): EEG discriminant analyses of mild head trauma. *Electroenceph. Clin. Neurophysiol.* 74, 94–106

Thatcher, R.W., Cantor, D.S., McAlaster, R., Geisler, F.H., Krause, P. (1990): Comprehensive prediction of outcome in head injured patients: Development of prognostic equations. *Ann. NY Acad. Sci.* (in press)

Thompson, J., Stewart, H. (1986): *Nonlinear dynamics and chaos.* New York: John Wiley & Sons

Wilder, C.S. (1976): Health Interview Survey. Rockville, MD: National Center for Health Statistics, Department of Health, Education and Welfare

Wilson, H.R., Cowen, J.D. (1972): Excitatory and inhibitory interactions in localized populations of model neurons. *J. Biophysics* 12, 1–24

Wilson, H.R., Cowen, J.D. (1973): A mathematical theory of the functional dynamics of cortical and thalamic nervous tissue. *Kybernetik* 13, 55–80

Wolf, A., Swift, J.B., Swinney, H.L., Vastano, J.A. (1985): Determining Lyapunov exponents from a time series. *Physica* 16D, 285–317